ORIGINAL RESEARCH

# Endothelial-Specific Loss of Sphingosine-1-Phosphate Receptor 1 Increases Vascular Permeability and Exacerbates Bleomycin-induced Pulmonary Fibrosis

Rachel S. Knipe[1,2,3], Jillian J. Spinney[1,2,3], Elizabeth A. Abe[1,2,3], Clemens K. Probst[4], Alicia Franklin[5], Amanda Logue[1,2,3], Francesca Giacona[1,2,3], Matt Drummond[1,2,3], Jason Griffith[1,3], Patricia L. Brazee[1,2,3], Lida P. Hariri[2,6], Sydney B. Montesi[1,2], Katherine E. Black[1,2,3], Timothy Hla[7], Andrew Kuo[7], Andreane Cartier[7], Eric Engelbrecht[8], Christina Christoffersen[9], Barry S. Shea[10], Andrew M. Tager[1,2,3†], and Benjamin D. Medoff[1,2,3]

[1]Division of Pulmonary and Critical Care Medicine, [2]Andrew M. Tager Fibrosis Research Center, [3]Center for Immunology and Inflammatory Diseases, [5]The MGH Institute of Health Professions, and [6]Department of Pathology, Massachusetts General Hospital and Harvard Medical School, Boston, Massachusetts; [4]Boston University School of Medicine, Boston University, Boston, Massachusetts; [7]Vascular Biology Program, Boston Children's Hospital and Harvard Medical School, Boston, Massachusetts; [8]University of Louisville School of Medicine, Louisville, Kentucky; [9]Department of Clinical Biochemistry, Rigshospitalet, and Department of Biomedical Sciences, University of Copenhagen, Copenhagen, Denmark; and [10]Division of Pulmonary, Critical Care, and Sleep Medicine, Rhode Island Hospital and Alpert Medical School, Providence, Rhode Island

ORCID ID: 0000-0002-4337-5748 (R.S.K.).

## Abstract

Idiopathic pulmonary fibrosis (IPF) is a chronic, progressive disease which leads to significant morbidity and mortality from respiratory failure. The two drugs currently approved for clinical use slow the rate of decline in lung function but have not been shown to halt disease progression or reverse established fibrosis. Thus, new therapeutic targets are needed. Endothelial injury and the resultant vascular permeability are critical components in the response to tissue injury and are present in patients with IPF. However, it remains unclear how vascular permeability affects lung repair and fibrosis following injury. Lipid mediators such as sphingosine-1-phosphate (S1P) are known to regulate multiple homeostatic processes in the lung including vascular permeability. We demonstrate that endothelial cell–(EC) specific deletion of the S1P receptor 1 (S1PR1) in mice (EC-*S1pr1*$^{-/-}$) results in increased lung vascular permeability at baseline. Following a low-dose intratracheal bleomycin challenge, EC-*S1pr1*$^{-/-}$ mice had increased and persistent vascular permeability compared with wild-type mice, which was strongly correlated with the amount and localization of resulting pulmonary fibrosis. EC-*S1pr1*$^{-/-}$ mice also had increased immune cell infiltration and activation of the coagulation cascade within the lung. However, increased circulating S1P ligand in ApoM-overexpressing mice was insufficient to protect against bleomycin-induced pulmonary fibrosis. Overall, these data demonstrate that endothelial cell S1PR1 controls vascular permeability in the lung, is associated with changes in immune cell infiltration and extravascular coagulation, and modulates the fibrotic response to lung injury.

**Keywords:** lung fibrosis; sphingosine-1-phosphate; sphingosine-1-phosphate 1 receptor; vascular permeability

Idiopathic pulmonary fibrosis (IPF) is a debilitating lung disease characterized by the progressive loss of lung function as a result of unrelenting scarring of the lungs. The overall prognosis in IPF is poor, with an average time to respiratory failure and death of

(Received in original form September 4, 2020; accepted in final form July 26, 2021)

†Deceased.

Supported by an American Thoracic Society/Scleroderma Foundation grant (R.S.K.) and National Institutes of Health grants K08HL140175 (R.S.K.) and R01HL133153 (B.D.M.).

Author Contributions: Conception and design: R.S.K., B.S.S., A.M.T., and B.D.M. Data acquisition: R.S.K., J.J.S., E.A.A., C.K.P., A.F., A.L., F.G., M.D., J.G., P.L.B., L.P.H., K.E.B., T.H., A.K., and A.C. Analysis and interpretation: R.S.K., T.H., E.E., B.S.S., and B.D.M. Drafting the manuscript: R.S.K. Revising the manuscript for important intellectual content: J.J.S., E.A.A., C.K.P, A.F., A.L., J.G., L.P.H., S.B.M., K.E.B., T.H., C.C., B.S.S., and B.D.M.

Correspondence and requests for reprints should be addressed to Rachel S. Knipe, M.D., Division of Pulmonary and Critical Care Medicine, 149 13th Street, Charlestown, MA 02129. E-mail: rknipe@mgh.harvard.edu.

This article has a data supplement, which is accessible from this issue's table of contents at www.atsjournals.org.

Am J Respir Cell Mol Biol Vol 66, Iss 1, pp 38–52, January 2022

Originally Published in Press as DOI: 10.1165/rcmb.2020-0408OC on August 3, 2021
Internet address: www.atsjournals.org

3–5 years from the time of diagnosis (1). In 2014, two drugs, nintedanib and pirfenidone, received FDA approval for patients with IPF after clinical trials demonstrated that these drugs slowed the rate of lung function decline (2, 3). However, there remains a great need for additional therapies that can halt and ultimately reverse established fibrosis. The development of novel effective treatments hinges on improved understanding of the biological processes that produce fibrosis and the molecular mechanisms that drive them.

IPF is believed to result from dysregulated wound repair following lung injury (4). One of the cardinal wound healing responses after any tissue injury is endothelial dysfunction, which leads to an increase in permeability of the tissue vasculature (5). There has been a long-standing appreciation that IPF patients have increased pulmonary vascular permeability, with higher permeability indices associated with worse outcomes (6). A study using inhaled technetium 99 m-labeled diethylenetriaminepentacetate ($^{99\ m}$Tc-DTPA) in patients with IPF demonstrated increased clearance times of the radiolabeled molecule, suggesting a disruption of the alveolar capillary barrier, which is associated with worse survival (7). In a more recent study, MRI imaging of the lung using an albumin-binding gadolinium probe demonstrated increased albumin extravasation in the lungs of patients with IPF as compared with healthy control subjects (8). Furthermore, electron microscopy studies performed on endothelial cells of alveolar capillaries in patients with interstitial lung disease, especially those with IPF, demonstrated increased fenestration, which correlated with the degree of interstitial fibrosis along the alveolar walls (9).

One of the main pathways regulating endothelial permeability is the interaction of a bioactive sphingolipid, sphinogosine-1-phosphate (S1P), with one of its cell surface G protein coupled receptors (GPCRs), S1PR1 (10). Interestingly, S1P levels have been shown to be elevated in serum and BAL fluid from patients with IPF (11). However, S1P can interact with five different receptors, S1PR1-S1PR5, on multiple different cell-types, resulting in different downstream effects. S1PR1 is the predominant receptor on lung endothelial cells, where the receptor can be activated by both local autocrine signaling as well as by circulating S1P. We have shown previously that pharmacologic functional antagonism of S1PR1 in mice, combined with a low dose of intratracheal bleomycin, resulted in exaggerated vascular leak and increased pulmonary fibrosis (12). However, S1PR1 is known to play a critical role in lymphocyte trafficking, and antagonism of S1PR1 on lymphocytes may have contributed to the development of pulmonary fibrosis in that model. It has also been shown previously that mice lacking plasma S1P have increased vascular permeability at baseline and in response to various edemagenic stimuli (13). However, the specific role that endothelial S1PR1 plays in the development of injury-induced vascular permeability and resultant fibrosis has not been well defined. Therefore, we employed a genetic approach to achieve an endothelial-specific reduction in *S1pr1* expression and to determine the specific role that endothelial S1PR1 plays in regulating endothelial permeability and pulmonary fibrogenesis.

In these studies, we found that genetic deletion of *S1pr1* from endothelial cells using an inducible Cre-recombinase system in mice led to increased vascular permeability even in the absence of lung injury. Following lung injury, mice with endothelial-specific deletion of *S1pr1* showed further increases in vascular permeability, as well as increased fibrosis. Our findings suggest that agonism of this specific ligand/receptor interaction on endothelial cells might be a novel and effective therapeutic strategy for the treatment of pulmonary fibrosis.

## Methods

### Mice

Mice with the sphingosine-1-phosphate receptor 1 (*S1pr1*) gene flanked by loxP sites (*S1pr1*$^{f/f}$) were provided by Dr. Jerold Chun (14). They were crossed with mice that express an inducible Cre recombinase under an endothelial cell-specific promoter (VECadherin-CreERT2), shared by Dr. Ralf Adams (15). Both mice were on a C57BL/6 background. Littermates with the *S1pr1* gene flanked by loxP sites but lacking the VECadherin-CreERT2 gene were used as control animals. Mice were treated with 200 mg/kg tamoxifen (Sigma) by oral gavage for 2 weeks (10 doses, Monday to Friday) beginning at age 4 weeks. Transgenic mice that overexpress apolipoprotein M (ApoM Tg$^{+}$) were developed and characterized by Dr. Christina Christofferson (16). Transgene-negative littermates were used as control animals. All mice were maintained in a specific pathogen–free (SPF) environment certified by the American Association for Accreditation of Laboratory Animal Care. All protocols performed were approved by the Massachusetts General Hospital Institutional Animal Care and Use Committee. All experiments used sex-matched male and female mice at 8 to 12 weeks of age.

### Gene Expression

Cells were sorted by flow cytometry and identified as endothelial cells (CD31$^{+}$CD45$^{-}$Epcam$^{-}$), epithelial cells (Epcam$^{+}$CD45$^{-}$CD31$^{-}$), or hematopoietic cells (CD45$^{+}$CD31$^{-}$Epcam$^{-}$). RNA was isolated from each cell group and quantitative PCR (qPCR) was performed to quantify *S1pr1* expression. Primers were obtained from MGH PrimerBank (https://pga.mgh.harvard.edu/primerbank/).

### Single-Cell RNA Sequencing Data

Seurat (17) objects were generated from single-cell RNA sequencing (scRNAseq) data deposited in Gene Expression Omnibus accessions GSE135893 (18) and GSE136831 (19) with associated metadata. The *subset* function was used to extract only cells annotated as vascular endothelial cells (vEC). Normalization was performed using the *NormalizeData* function. vEC were merged using the *FindIntegrationAnchors* and *IntegrateData* functions with *dims = 1:50*. To identify vEC clusters, the top 3,000 transcripts showing cell-to-cell variation were used in the *FindVariableFeatures* function with the *vst* option, and the resolution parameter of *FindClusters* set to 0.2. UMAP, violin plot, and dot plot visualizations were generated using the functions *RunUMAP*, *DimPlot*, *VlnPlot*, and *DotPlot*. *S1pr1* expression was queried using the *AverageExpression* function with *features* = "*S1PR1*".

### Flow Cytometry

Mouse lungs were digested using DNase and Liberase (Sigma) to generate a single cell suspension and then stained with fluorescent antibodies. S1pr1 antibody (R&D) was used to label S1pr1 expressing mouse lung cells. To identify macrophage/monocyte

subpopulations of lung cells by flow cytometry, the following antibody panel was used: CD45.2$^+$ (AF700) injected intravenously prior to harvest, Viability (APC-Cy7), Siglec F$^+$ (PE), CD11c$^+$ (BV605), MHCII$^+$ (PE-Cy7), CD64$^+$ (APC), Ly6C$^+$ (PerCyP Cy5.5), CD103$^+$ (BV421), CD11b$^+$ (BV396), Ly6G$^+$ (FITC). To identify lymphocyte subpopulations of lung cells by flow cytometry, the following antibody panel was used: CD45.2$^+$ (AF700) injected intravenously prior to harvest, Viability (APC-Cy7), CD3$^+$ (BV396), NK1.1$^+$ (FITC), TCR-B (BV421), CD19$^+$ (PE), TCR-GD (PerCP-Cy5.5), CD4$^+$ (BV605), CD8$^+$ (PE-Cy7), FoxP3$^+$ (APC).

### Immunoblotting

Proteins in whole lung lysates were resolved by SDS-PAGE and then transferred to polyvinylidene difluoride membranes using the NuPAGE electrophoresis and transfer systems (Life Technologies) under reducing conditions. After blocking with 5% milk, membranes were incubated with anti-S1pr1 antibody (H60) followed by horseradish peroxidase-conjugated secondary antibodies (Cell Signaling), and then visualized with Amersham ECL chemiluminescent substrate (GE Healthcare). Membranes were then stripped and similarly re-probed for GAPDH (Cell Signaling) as a loading control. Densitometry of the immunoblots was performed using Image J software (NIH).

### Peripheral Blood Counts

Mouse peripheral blood was collected by facial venous puncture. Blood was collected in EDTA containing microtainer tubes (BD), and complete blood count, including leukocyte differential, was performed through the MGH Center for Comparative Medicine Animal Laboratory.

### Bleomycin-induced Pulmonary Fibrosis

Fibrosis was induced by single-dose intratracheal (IT) injection of bleomycin (Fresenius Kabi) at a standard dose of 1.0 units/kg and also at a reduced dose of 0.5 units/kg, and quantified by measuring hydroxyproline content, per our usual methods (20).

### Assessment of Vascular Permeability

Lung vascular permeability was assessed by measuring BAL total protein concentration and performing Evans blue dye assays by published methods (12, 20), as described in online supplemental methods. BAL total protein quantification was performed using a BCA assay (Pierce).

### Histological Analysis and Immunohistochemistry

After the right ventricle and pulmonary vasculature were flushed with 10 ml cold PBS, lungs were inflated with 10% buffered formalin at 25 cm $H_2O$ for 15 minutes, excised and fixed in 10% formalin for 24 hours, and then embedded in paraffin. Paraffin-embedded 5-μm sections were stained with hematoxylin and eosin or Masson's trichrome stains. FITC-Albumin was injected by tail vein prior to euthanasia of the animal. Bleomycin-treated mouse lungs were inflated ex-vivo and fixed with 4% PFA for 15 minutes prior to sectioning and staining for S1pr1 (H60). Human lungs were fixed with 10% buffered formalin per MGH pathology protocol and processed in paraffin prior to staining for S1pr1 (H60) and VE-Cadherin (R&D).

### Coagulation Studies

Extravascular coagulation was quantified using a D-dimer ELISA assay (Asserachrom) performed on BAL and lung tissue homogenates obtained from mice after intravenous flush of the pulmonary vasculature with sterile saline.

### Plasma Sphingolipid Quantification

Plasma was collected from wild-type mice at 0, 3, 7, 10, and 14 days after IT bleomycin injection (1.0 units/kg) in EDTA containing syringes and tubes. Mouse plasma was quantified by mass spectroscopy analysis as previously described (21). Plasma was separately collected from patients with IPF ($n = 30$) and healthy volunteers ($n = 30$) of similar ages through the MGH Biorepository of Interstitial Lung Diseases under an institutional review board–approved protocol with all subjects providing informed consent. Human plasma was sent for S1P quantification to Dr. Timothy Hla's lab (22).

### Human Lung Tissue Analysis

Through the Massachusetts General Hospital ILD Translational Research Program, IPF lung tissue was collected from patients undergoing lung transplantation at time of explant. Healthy lung tissue for control subjects was collected from patients undergoing lung biopsy for non-fibrotic lesions. The excess tissue from around the biopsy site was obtained for histology.

### Statistical Analysis

Data are reported as mean ± SD. In all experiments, differences between groups were analyzed for statistical significance with two-tailed Student's *t* tests, using GraphPad Prism software. $P \leq 0.05$ was considered significant for all comparisons.

## Results

### Endothelial-Specific *S1pr1* Deletion Mice Are Viable and Phenotypically Normal at Baseline but Have Increased Pulmonary Vascular Permeability

Tamoxifen was administered by oral gavage to S1pr1$^{f/f}$ × VECad-CreERT2 mice beginning at 4 weeks of age to induce deletion of the *S1pr1* gene in endothelial cells (EC-*S1pr1*$^{-/-}$ mice), and to S1pr1$^{f/f}$ littermates as controls (14). To confirm cell-specific deletion of *S1pr1*, fluorescence-activated cell sorting was performed to isolate CD31$^+$ endothelial cells, CD45$^+$ hematopoietic cells, and Epcam$^+$ epithelial cells. By qPCR, *S1pr1* mRNA expression was reduced by 85% in endothelial cells from EC-*S1pr1*$^{-/-}$ mice compared with control mice (Figure 1A). Of note, *S1pr1* expression was not reduced in the other cell populations examined, including hematopoietic cells, which are known to express *S1pr1*, confirming that VECad-CreERT2 is endothelial cell–specific (Figures 1B and 1C). In addition, we measured the surface expression of S1PR1 on CD31$^+$ endothelial cells by flow cytometry and confirmed reduced protein expression in pulmonary endothelial cells isolated from EC-*S1pr1*$^{-/-}$ mice (Figure 1D). Finally, immunofluorescent staining of EC-*S1pr1*$^{-/-}$ mouse lungs and intact littermate control lungs demonstrates reduced staining for S1PR1 on VE-Cadherin (CDH5)$^+$ endothelial cells (Figure 1E). Evans blue dye assays demonstrated increased pulmonary vascular permeability in EC-*S1pr1*$^{-/-}$ mice compared with littermate controls (Figure 2A). However, these mice were viable and phenotypically normal, and their lungs appeared normal by hematoxylin and eosin and Masson's trichrome staining, suggesting that under homeostatic conditions this increased vascular permeability is well tolerated (*see* Figure E1A in the data supplement). Lymphocyte *S1pr1* is required for normal lymphocyte egress from secondary lymphoid organs, and

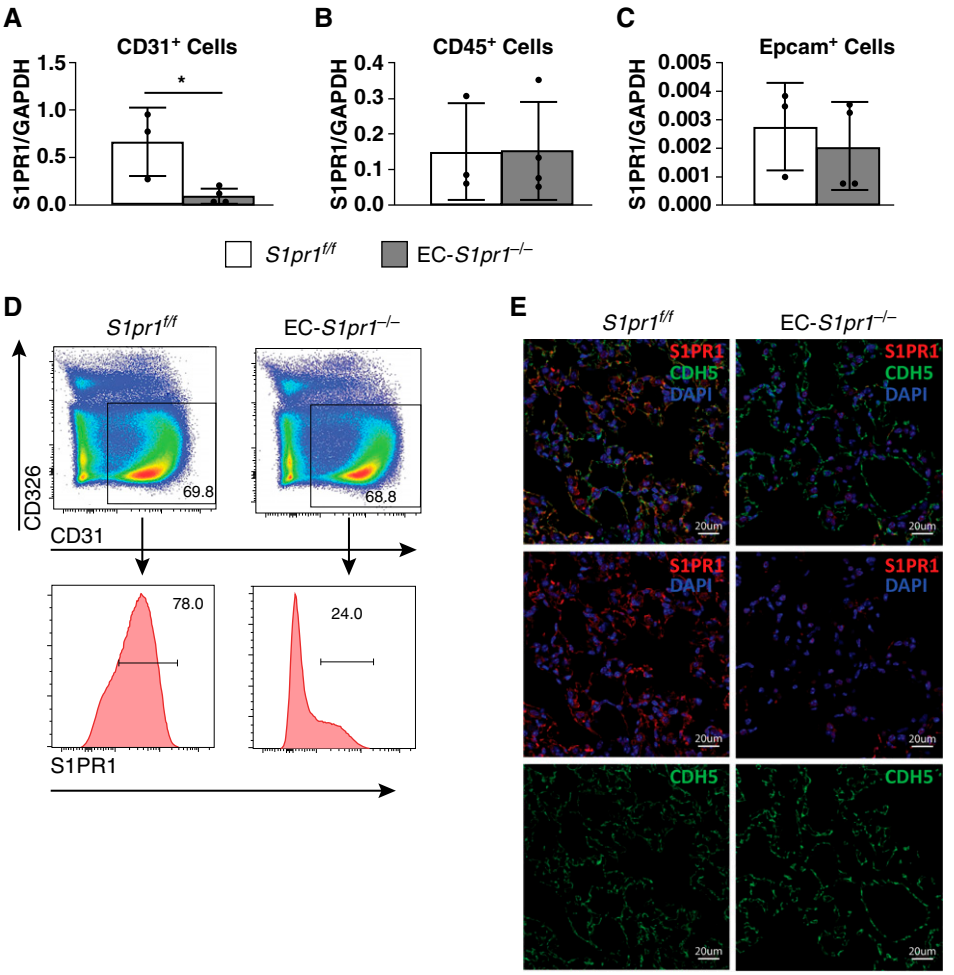


**Figure 1.** Endothelial-specific *S1pr1* expression is reduced in EC-*S1pr1*$^{-/-}$ mice. *S1pr1* mRNA expression in isolated (*A*) endothelial cells (CD31$^{+}$), (*B*) hematopoietic cells (CD45$^{+}$), and (*C*) epithelial cells (Epcam$^{+}$). $n = 3$ mice per group. (*D*) Flow cytometry of mouse lung endothelial cells in EC-*S1pr1*$^{-/-}$ mice (S1PR1$^{f/f}$ × VECad-CreERT2) compared with littermate controls (*S1pr1*$^{f/f}$). (*E*) Immunofluorescence confirming deletion of EC S1PR1 after tamoxifen. Representative images shown; $n = 3$ mice per group. *$P < 0.05$ comparing expression of *S1pr1* in EC-*S1pr1*$^{-/-}$ mice as compared with *S1pr1*$^{f/f}$ mice. Scale bars, 20 μm.

nonselective *S1pr1* inhibition is known to induce peripheral lymphopenia. Peripheral blood lymphocyte counts were quantified after tamoxifen administration and showed that EC-*S1pr1*$^{-/-}$ mice had intact peripheral lymphocyte counts (Figures E1B and E1C).

### Standard-Dose Bleomycin Increases Pulmonary Vascular Permeability in Endothelial-Specific *S1pr1* Deletion Mice

We administered a standard dose of bleomycin (1.0U/kg) intratracheally (IT) to induce lung injury. Seven days after the bleomycin challenge, both control and EC-*S1pr1*$^{-/-}$ mice showed an increase in vascular permeability compared with Day 0 (baseline), but the EC-*S1pr1*$^{-/-}$ mice showed exaggerated vascular permeability compared with controls (Figures 2A and 2B). Additionally, EC-*S1pr1*$^{-/-}$ mouse lungs appeared to have increased intraalveolar edema fluid and fibrin deposition, indicated by increased red Masson's trichrome staining on histology, compared with littermate controls (Figure 2C). There was no change in collagen content or fibrosis in the lungs of EC-*S1pr1*$^{-/-}$ mice on Day 7 after standard dose bleomycin (Figures E1D and E1E), which suggests that the fibrotic response was not accelerated by the increase in permeability. There was increased mortality in the EC-*S1pr1*$^{-/-}$ mice by Day 14 after standard-dose bleomycin challenge (1.0 U/kg), which precluded our ability to accurately assess fibrosis at Days 14 to 21 (Figure 2D).

### Mice with Endothelial-Specific *S1pr1* Deletion Have Increased Fibrosis in Response to Low-Dose Bleomycin

Given the increased mortality in EC-*S1pr1*$^{-/-}$ mice with the standard dose of bleomycin, we tested a lower dose of bleomycin (0.5U/kg). Despite the lower dose of bleomycin, there was still an increase in mortality in EC-*S1pr1*$^{-/-}$ mice compared with littermate controls (Figure 3A), but enough mice survived for 21 days to allow for analysis. As an initial marker of injury and vascular permeability after low-dose bleomycin, total protein in the BAL fluid was quantified at multiple time points. Both control and EC-*S1pr1*$^{-/-}$ mice showed an increase in BAL total protein after bleomycin challenge; however, by Day 7, EC-*S1pr1*$^{-/-}$ mice showed significantly more BAL total

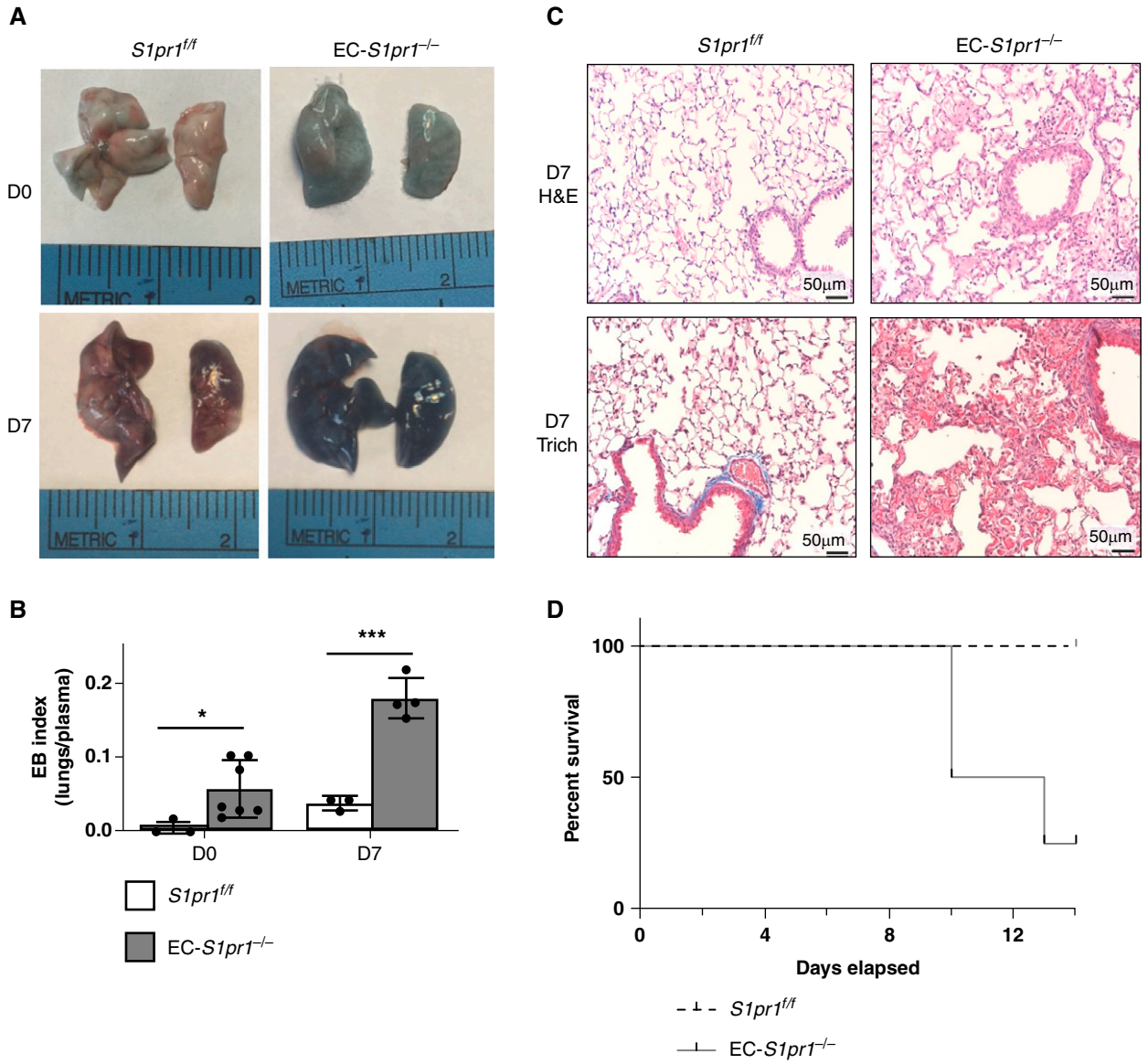


**Figure 2.** Standard-dose bleomycin increases pulmonary vascular permeability in EC-*S1pr1*$^{-/-}$ mice. (*A*) Evans blue dye assay was performed on Day 0 and Day 7 after standard-dose intratracheal (IT) bleomycin (1.0 U/kg). (*B*) Quantification of vascular permeability was calculated as an Evans blue (EB) index defined as the ratio of lung Evans blue to plasma Evans blue. $n = 3$–7 mice per group. (*C*) Hematoxylin and eosin and Masson's trichrome staining of lungs was performed on Day 7 after standard dose bleomycin. Representative images are shown from $n = 3$ mice per group. Scale bars, 50 μm. (*D*) Survival of mice receiving standard-dose (1.0 U/kg) bleomycin. $n = 5$ mice per group. $^{*}P < 0.05$ comparing survival of EC-*S1pr1*$^{-/-}$ mice to littermate controls *S1pr1*$^{f/f}$. $^{***}P < 0.001$ comparing EB index in EC-*S1pr1*$^{-/-}$ mice to littermate controls *S1pr1*$^{f/f}$. H&E = hematoxin and eosin; Trich = trichrome.

protein compared with littermate controls, and this persisted up to 21 days after bleomycin challenge (Figure 3B). Histology of the lungs at Day 21 demonstrated increased fibrosis by hematoxylin and eosin staining and increased collagen deposition by Masson's trichrome staining in EC-*S1pr1*$^{-/-}$ mice (Figure 3C). Fibrosis was quantified by hydroxyproline assay at days 0, 7, 14, 21, and 42 after bleomycin challenge and was found to be significantly increased in EC-*S1pr1*$^{-/-}$ mice at Days 14 and 21 compared with littermate controls (Figure 3D**).** There was a trend to increased fibrosis at Day 42 in the EC-*S1pr1*$^{-/-}$ mice. Ashcroft scoring also demonstrated increased fibrosis in EC-*S1pr1*$^{-/-}$ mice at Day 14 and 21 as compared with intact littermate controls (Figure 3E). Low-dose bleomycin was insufficient to induce fibrosis in the control mice. However, the combination of increased vascular permeability seen with endothelial *S1pr1* deletion and low-dose bleomycin injury was able to induce pulmonary fibrosis.

***Vascular permeability co-localized with fibrosis in mice lacking endothelial S1pr1.*** Two weeks after IT bleomycin challenge, when fibrosis had been established, EC-*S1pr1*$^{-/-}$ mice and littermate controls were injected intravenously with FITC-labeled albumin. Lungs were harvested, fixed, and sectioned

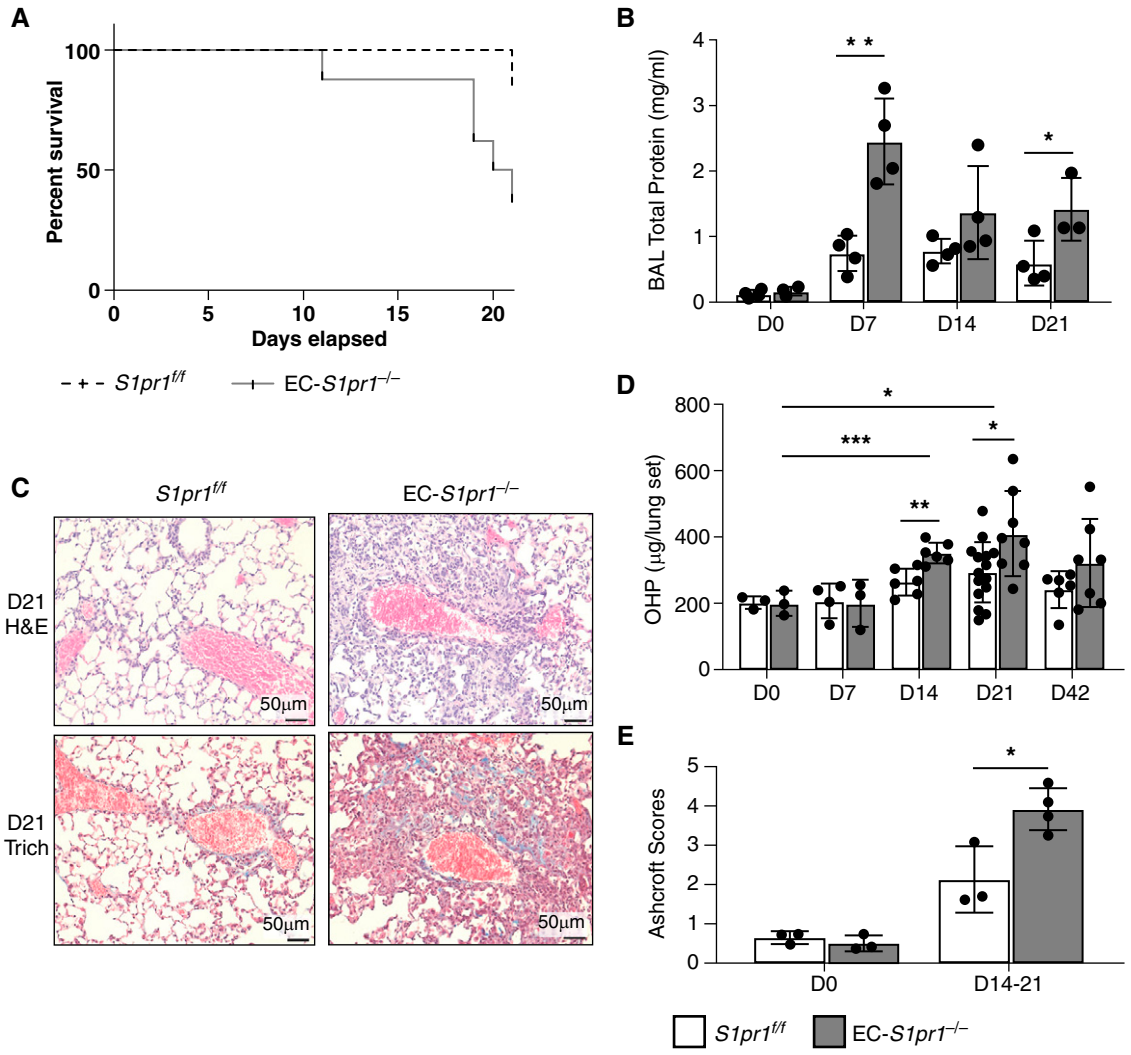


**Figure 3.** Low-dose bleomycin induces fibrosis in EC-*S1pr1*$^{-/-}$ mice. (*A*) Survival of mice receiving low-dose (0.5 U/kg) bleomycin. $n = 5$ mice per group. (*B*) Total protein content in the BAL was quantified at Days 0, 7, 14, and 21 after low-dose bleomycin. BAL from EC-*S1pr1*$^{-/-}$ mice was compared with intact littermate controls *S1pr1*$^{f/f}$. $n = 3$–5 mice per group. (*C*) Hematoxylin and eosin and Masson's trichrome staining of lungs were performed on Day 21 after low-dose bleomycin. Representative images are shown from $n = 3$ mice per group. Scale bars, 50 μm. (*D*) Fibrosis was quantified at Days 0, 7, 14, 21, and 42 after low-dose IT bleomycin by measuring hydroxyproline levels in the mouse lungs. $n = 3$–15 mice per group. (*E*) Ashcroft scoring performed on trichrome stained lung sections from EC-*S1pr1*$^{-/-}$ mice at Days 0 and 14 or 21 was compared with intact littermate controls *S1pr1*$^{f/f}$. $n = 3$–4 mice per group. $^{*}P < 0.05$, $^{**}P < 0.01$, and $^{***}P < 0.001$ for comparisons of total protein or hydroxyproline in EC-*S1pr1*$^{-/-}$ mice compared with intact littermate control mice *S1pr1*$^{f/f}$. OHP = hydroxyproline.

sequentially. Lung tissue sections were stained with Masson's trichrome stain for visualization of fibrosis and with anti-FITC antibody for visualization of albumin leakage. In EC-*S1pr1*$^{-/-}$ mice, albumin extravasation was seen diffusely but was most heavily concentrated in the perivascular regions of the lung (Figure 4A). Interestingly, in sequential slices, collagen deposition colocalized in the perivascular regions where endothelial barrier function was disrupted, and permeability was increased.

***Endothelial-specific* S1pr1 *deletion leads to increased extravascular coagulation.*** Intraalveolar and total lung extravascular coagulation was quantified by measuring D-dimer levels in the BAL and lung tissue, respectively, of EC-*S1pr1*$^{-/-}$ mice and intact littermate controls. We have previously shown that lung D-dimer levels correlated with fibrin deposition, as quantified by molecular imaging with magnetic resonance imaging (MRI) (23). BAL D-dimer was increased in both groups 7 days following low-dose IT bleomycin challenge, but levels declined by Day 14 in control mice, whereas in EC-*S1pr1*$^{-/-}$ mice, D-dimer levels remained persistently elevated at Days 14 and 21 (Figure 4B). A similar increase in D-dimer levels was seen in whole lung homogenates of EC-*S1pr1*$^{-/-}$ mice compared with intact littermate controls at 7, 14, and 21 days after bleomycin challenge. Interestingly, the lung D-dimer levels of control mice did not show a significant increase, demonstrating that a

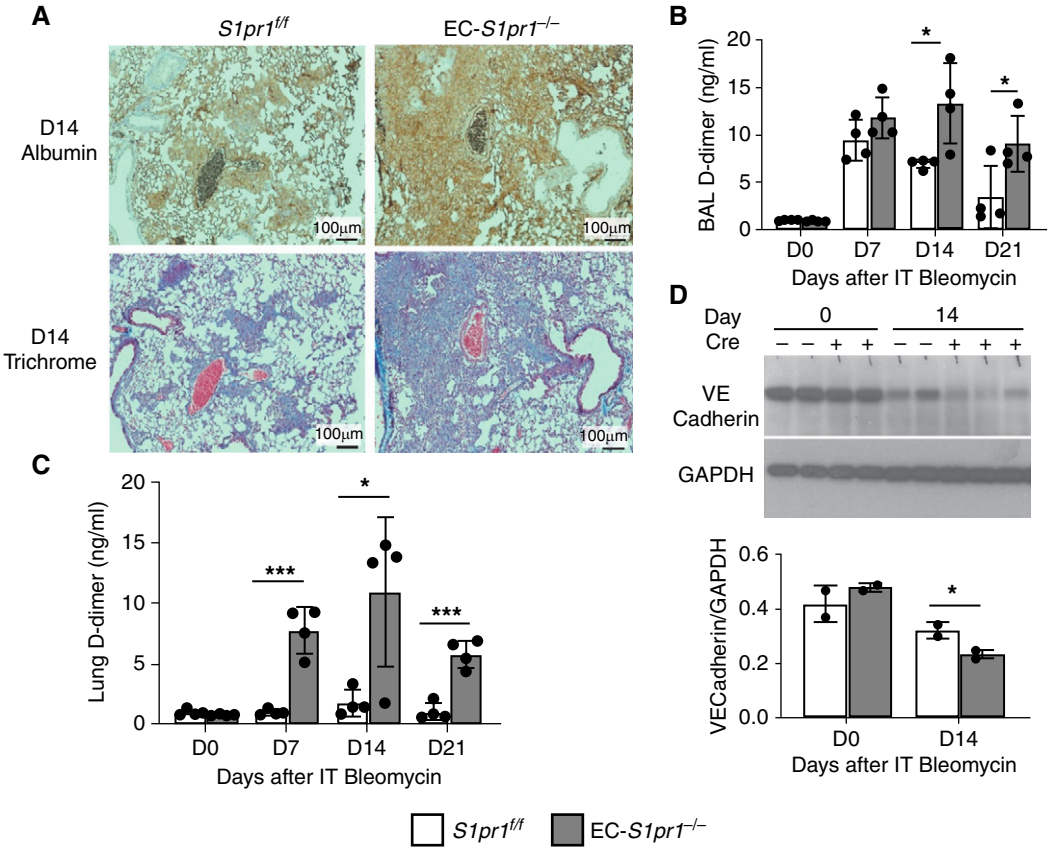


**Figure 4.** Endothelial-specific *S1pr1* deletion leads to reduced intercellular junction proteins and increased extravascular coagulation. (*A*) Mice were injected with FITC-labeled albumin to identify albumin extravasated into the lung tissue after bleomycin. Sequential sectioning and staining of the lung tissue were performed with Masson's trichrome stain. Representative images are shown from $n = 3$ mice per group. Scale bars, 100 μm. (*B*) D-dimer ELISA was performed on BAL fluid collected from mice on days 0, 7, 14, and 21 after low-dose IT bleomycin (0.5 U/kg). $n = 4$ mice per group. (*C*) D-dimer ELISA was performed on homogenized lung tissue collected from mice on days 0, 7, 14, and 21 after low-dose IT bleomycin (0.5 U/kg). $n = 4$ mice per group. (*D*) Junctional proteins were assessed through immunoblotting for VE-Cadherin in lung tissue homogenates harvested at days 0 and 14 after low-dose bleomycin challenge. Densitometry was performed to quantify differences in protein expression at each time point. $n = 2$–3 mice per group. $^{*}P < 0.05$ and $^{***}P < 0.001$ for comparisons of D-dimer in the BAL and lung tissue of EC-*S1pr1*$^{-/-}$ mice as compared with intact littermate controls *S1pr1*$^{f/f}$.

single low-dose injection of bleomycin was insufficient to induce tissue coagulation in the absence of impaired permeability (Figure 4C).

***Increased vascular permeability was associated with reduced endothelial junctional protein expression.*** S1P/S1PR1 signaling on endothelial cells induces intracellular cytoskeletal rearrangements, tethering actin cortical ring structures to intercellular adherens junction proteins. With the endothelial cell deletion of *S1pr1*, we looked for changes in these structural protein complexes that regulate EC barrier function. Immunoblotting for the adherens junction protein VE-Cadherin showed a reduction in protein levels in lung homogenates from EC-*S1pr1*$^{-/-}$ mice at Day 14 after IT low-dose bleomycin compared with intact littermate controls (Figure 4D). This fits with previous data suggesting that S1PR1 is important for both regulating assembly of the adherens junction and also the expression of its components (24) and supports the hypothesis that EC barrier function was disrupted in the EC-*S1pr1*$^{-/-}$ mice.

***Increased immune cell populations in the BAL of mice lacking endothelial* S1pr1 *after bleomycin.*** Flow cytometry was performed on the BAL and lung tissue collected from EC- *S1pr1*$^{-/-}$ and control mice at Days 0 and 7 after standard dose to look for differences in immune cell infiltration in the context of increased vascular permeability. Gating strategies are shown in Figures E2A–E2B. Overall, there was an increase in total cells in the BAL after bleomycin challenge compared with baseline, with EC-*S1pr1*$^{-/-}$ mice showing an even greater increase compared with controls (Figure 5A). In the BAL at Day 7, EC-*S1pr1*$^{-/-}$ mice had preserved alveolar macrophage numbers as compared with controls and increased numbers of dendritic cells, natural killer (NK) cells, monocyte derived dendritic cells (DCs), inflammatory monocytes, $CD4^{+}$ and $CD8^{+}$ T cells, and T regulatory cells (Figures 5B–5I). There was no difference in the number of B cells, gamma delta T cells, eosinophils, and neutrophils in the BAL between the two groups of mice (Figures 5J–5M). There was a reduction in the total number of cells in the lung tissue at Day 7 after IT bleomycin challenge with no difference in the number

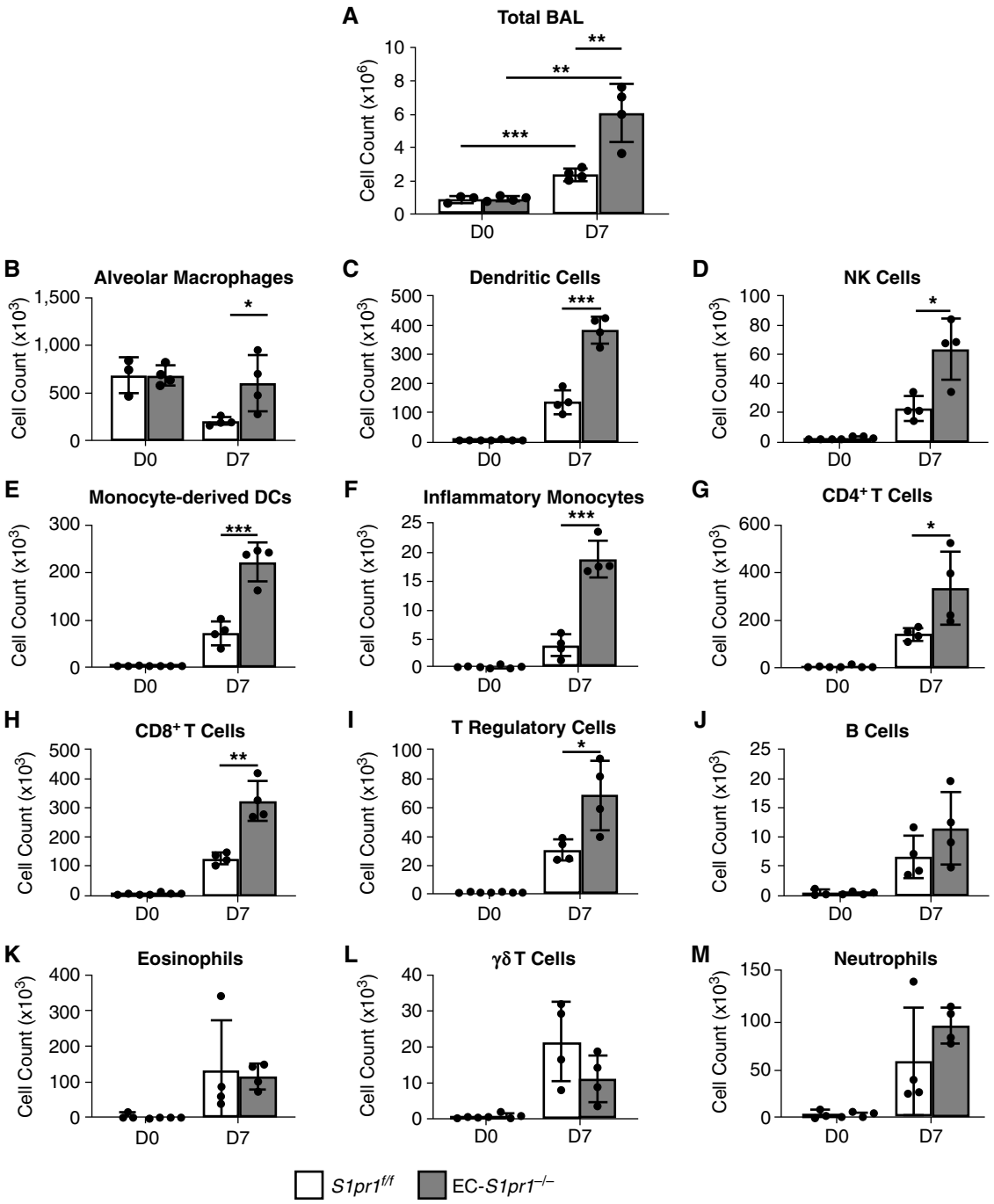


**Figure 5.** Immune cell populations in the BAL of mice lacking endothelial *S1pr1* after bleomycin. (*A*) Total cell counts were quantified from BAL obtained on Day 0 and Day 7 after low-dose IT bleomycin. $n = 3$–4 mice per group. Flow cytometry was performed on BAL collected 7 days after bleomycin challenge in EC-*S1pr1*$^{-/-}$ and control mice to assess the number of (*B*) alveolar macrophages, (*C*) dendritic cells, (*D*) NK cells, (*E*) monocyte-derived dendritic cells (DCs), (*F*) inflammatory monocytes, (*G*) CD4$^+$ T cells, (*H*) CD8$^+$ T cells, and (*I*) T regulatory cells. In contrast, no differences were detected in the quantities of BAL (*J*) B cells, (*K*) eosinophils, (*L*) γδ T cells, or (*M*) neutrophils. $n = 3$–4 mice per group. *$P < 0.05$, **$P < 0.01$, and ***$P < 0.001$ for comparisons of BAL cells in EC-*S1pr1*$^{-/-}$ mice as compared with intact control mice *S1pr1*$^{f/f}$. γδ T cells = GD T cells.

of cells between the groups (Figure E3A). There was an increase in alveolar macrophages in the lungs at baseline (Figure E3B) and an increase at Day 7 in the inflammatory monocytes in the lungs of EC-*S1pr1*$^{-/-}$ mice compared with controls (Figure E3C). There were no differences in any of the other immune cell populations in the lung tissue of mice at baseline or at Day 7 after IT bleomycin (Figure E4).

***Endothelial* S1pr1 *deletion is insufficient to induce fibrosis in the absence of lung injury.*** Because increased vascular permeability was observed in EC-*S1pr1*$^{-/-}$ mice at baseline, we asked

whether a persistent increase in permeability could induce fibrosis by itself, even in the absence of lung injury. To address this question, tamoxifen was administered to both EC-*S1pr1*$^{-/-}$ mice and littermate controls, and then the mice were maintained for 6 months. At this time point, there was no difference in overall health of the EC-*S1pr1*$^{-/-}$ mice. The deletion of *S1pr1* persisted at 6 months as measured by flow cytometry (data not shown). There was no clear histological evidence of pulmonary fibrosis (Figure 6A), and quantification of lung hydroxyproline levels confirmed no change in lung collagen content in the EC-*S1pr1*$^{-/-}$ mice relative to controls (Figure 6B). BAL total protein levels were similar in EC-*S1pr1*$^{-/-}$ mice compared with intact controls at baseline and 6 months after tamoxifen (Figure 6C). Furthermore, BAL and lung D-dimer levels were not elevated in EC-*S1pr1*$^{-/-}$ mice compared with intact controls (Figures 6D–6E). These results demonstrate that increased lung vascular permeability is well tolerated under homeostatic conditions and is insufficient to induce fibrosis in the absence of lung injury.

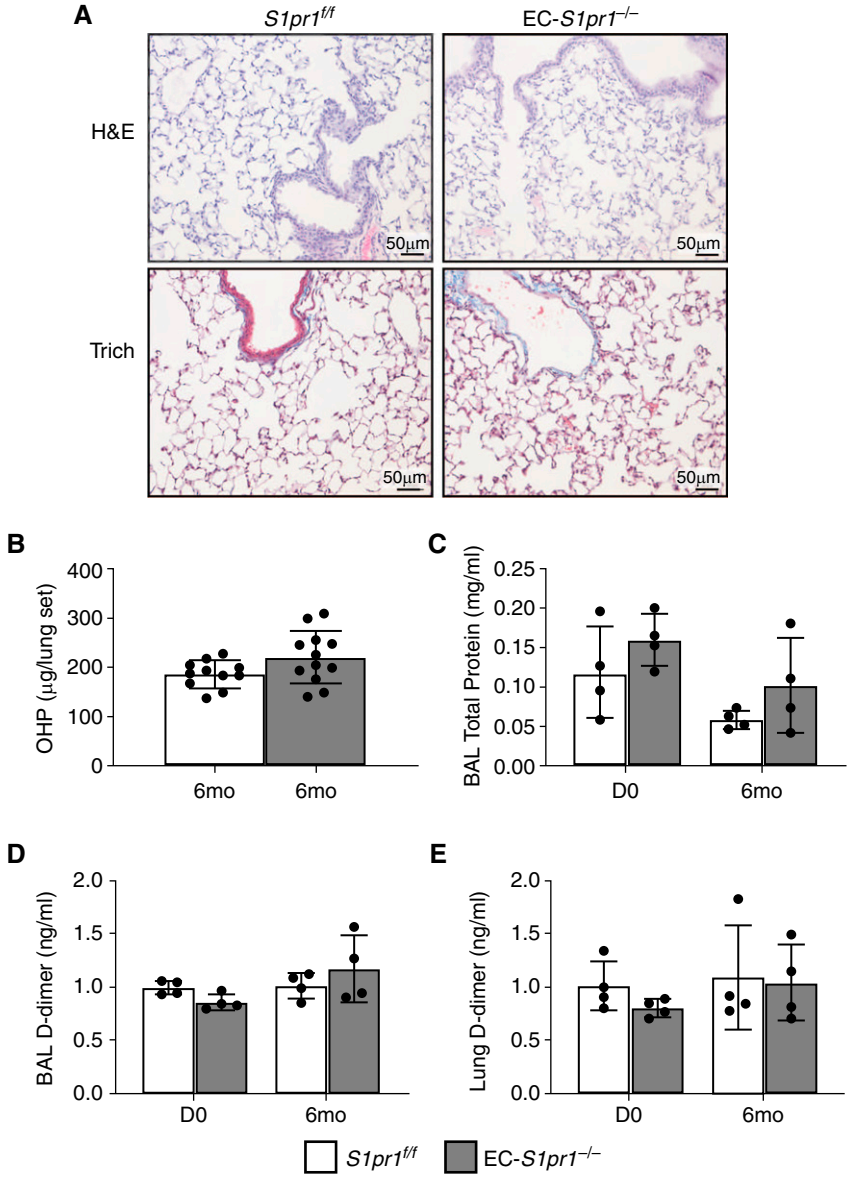


**Figure 6.** Endothelial *S1pr1* deletion is insufficient to induce fibrosis in the absence of lung injury. (*A*) For longitudinal studies, mice were treated with tamoxifen to induce EC-*S1pr1* deletion and then maintained in the mouse facility for 6 months. After 6 months, hematoxylin and eosin and Masson's trichrome staining were performed on lung histology from EC-*S1pr1*$^{-/-}$ mice and littermate controls *S1pr1*$^{f/f}$. Representative images are shown from $n = 3$ mice per group. Scale bars, 50 μm. (*B*) OHP assay was performed on lung tissue from mice after 6 months. $n = 11$–12 mice per group. (*C*) Total protein in the BAL fluid of mice after 6 months was compared. $n = 4$ mice per group. (*D*) BAL D-dimer levels were measured by ELISA. $n = 4$ mice per group. (*E*) Lung D-dimer levels were measured by ELISA. $n = 4$ mice per group.

***Bleomycin-induced lung injury reduces endothelial cell populations in the lung.*** We were interested in whether bleomycin-induced lung injury and fibrosis affected S1P/S1PR1 expression in the mouse lung. C57BL/6 wild-type (WT) mice were used to assess S1PR1 expression levels in the context of lung injury. Total lung S1PR1 expression in WT mice was quantified over 14 days after a standard-dose IT bleomycin challenge. There was a reduction in S1PR1 protein expression in lung tissue homogenates from WT mouse lungs between Days 1 and 14 (Figure 7A). Flow cytometry was performed on single cell suspensions of lung from WT-naive mice at baseline and on Days 7 and 14 after IT bleomycin to compare endothelial surface expression of S1PR1. There was a decrease in CD31$^+$ cells after bleomycin challenge (Figure 7B). However, S1PR1 levels on individual CD31$^+$ cells were increased after bleomycin, as seen by an increased mean fluorescent intensity (MFI) by flow cytometry (Figures 7C–7E). Thus, the loss of S1PR1 protein expression appears to be due to a reduction in total CD31$^+$ endothelial cells. It is not clear from this data whether the endothelial cells have undergone apoptosis or a phenotypic change as a result of bleomycin injury, resulting in a loss of CD31$^+$ surface expression. Endogenous S1P ligand levels were also quantified in the plasma of WT mice over the 14-day time course, and there was no difference in circulating ligand (Figure 7F). Immunofluorescent costaining for the endothelial marker CDH5 and S1PR1 was performed on WT mouse lungs harvested at Days 0 and 14 after IT bleomycin. In the EC-*S1pr1*$^{-/-}$ mice, the fibrotic regions had a disrupted endothelial barrier, as noted by reduced CDH5 expression (Figure 7G, white box). These same regions had reduced S1PR1 staining. There was some noncellular intraalveolar staining of S1PR1, which was nonspecific, but one possibility could be

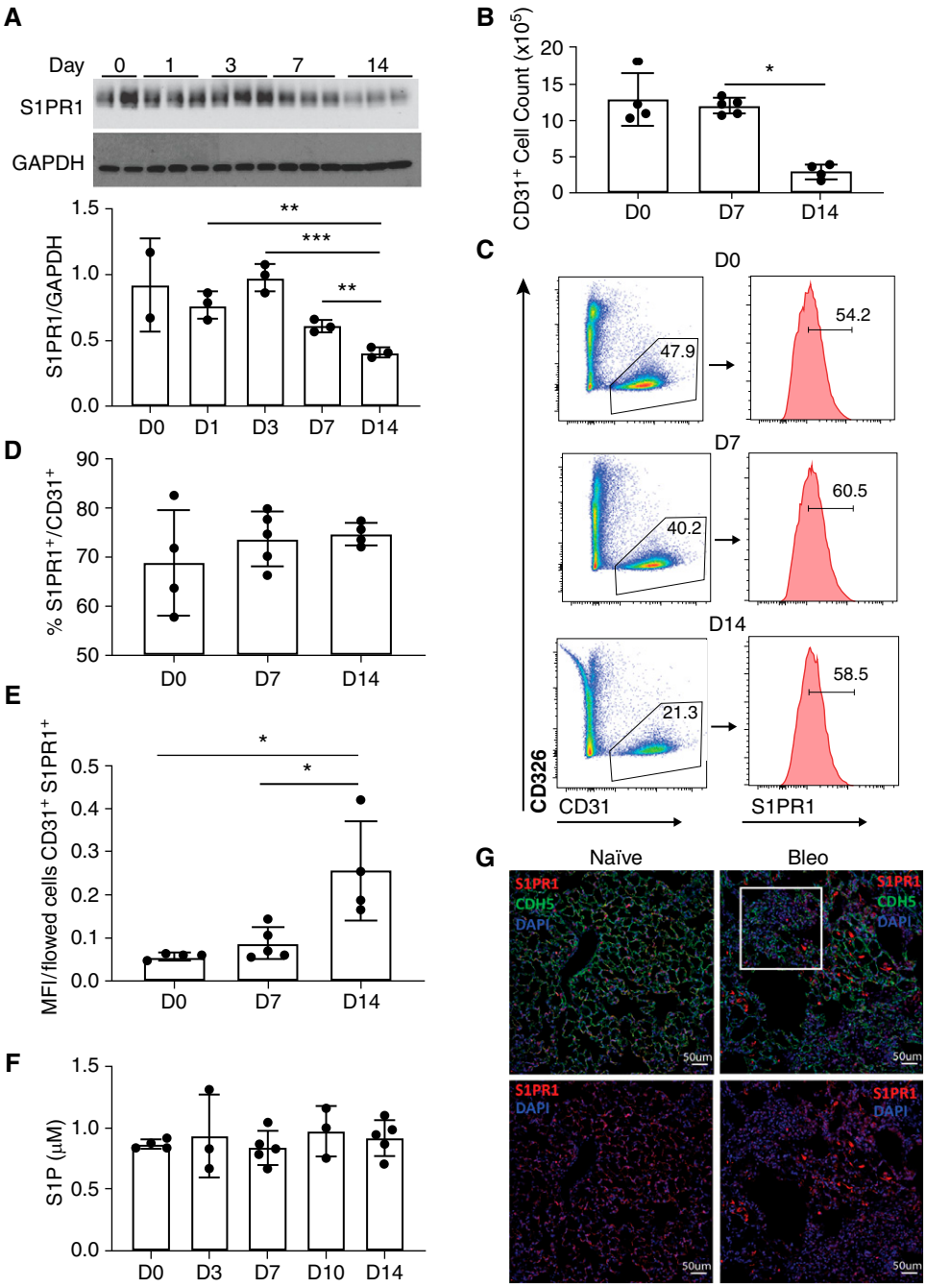


**Figure 7.** Bleomycin-induced lung injury reduces endothelial cell populations in the lung. (*A*) Immunoblotting was performed using protein from lung homogenates of C57BL/6 wild-type mice (WT) at Days 0, 1, 3, 7, and 14 after IT bleomycin (0.5 U/kg). Blots were probed for S1PR1, and protein expression levels were compared using GAPDH as a loading control. $n = 2$–3 mice per group. Densitometry was performed using Image J software (NIH). (*B*) Flow cytometry to identify $CD31^+$ cells was performed on lung tissue from WT mice on Days 0, 7, and 14 after standard-dose IT bleomycin. $n = 4$ mice per group. (*C*) Flow cytometry of $CD31^+$ cells expressing S1PR1. $n = 4$ mice per group. (*D*) The percentage of endothelial cells expressing S1PR1 at each time point after bleomycin was quantified. (*E*) Mean fluorescence intensity of S1PR1 in $CD31^+$ cells after bleomycin was quantified. (*F*) Plasma S1P levels in WT mice were quantified at Days 0, 3, 7, 10, and 14 after IT bleomycin. $n = 3$–4 mice per group. (*G*) Immunoflourescence co-staining on lungs from naive and bleomycin treated mice at Day 14 was performed for S1PR1 (red), endothelial CDH5/VE-cadherin (green), and nuclear DAPI (blue). White box indicates a fibrotic region. Scale bars, 50 μm. $^*P < 0.05$, $^{**}P < 0.01$, and $^{***}P < 0.001$ for comparisons of cells in WT mice at various time points after bleomycin injury.

apoptotic endothelial cells filling the alveolar spaces.

***Overexpression of plasma S1P chaperone is insufficient to protect mice from bleomycin-induced pulmonary fibrosis.*** Given that blocking S1P/S1PR1 signaling by knocking out S1PR1 expression led to increased vascular permeability and fibrosis in the IT bleomycin model, we next asked whether enhancing S1P/S1PR1 signaling could have protective effects. Mice that overexpress an S1P chaperone protein, apolipoprotein M (ApoM) (ApoM $Tg^+$) (16), have been shown to be protected in a liver model of fibrosis (25). In addition, plasma from these mice has been shown to prevent acid-induced fibrosis in the lungs of aged mice (26). We treated ApoM $Tg^+$ mice with a standard-dose IT bleomycin, assessed vascular permeability at Day 7 after IT bleomycin injury, and found no difference between the ApoM $Tg^+$ mice and controls (Figures 8A–8B). Total protein levels in the BAL fluid at Day 14 were compared, and no difference was found between the ApoM $Tg^+$ mice and controls (Figure 8C). Mouse lungs were stained for collagen deposition with Masson's trichrome staining, and patchy areas of fibrosis were noted in both ApoM $Tg^+$ mice and controls (Figure 8D). Pulmonary fibrosis was quantified by hydroxyproline assay at Day 14 after IT bleomycin, and there were no differences in fibrosis between ApoM $Tg^+$ and control mice (Figure 8E). We confirmed that ApoM $Tg^+$ mice had threefold higher circulating levels of S1P in the plasma as their littermate controls at baseline, and despite a persistent increase at both Days 7 and 14 after IT bleomycin, there was no protection from vascular permeability at Day 7 or fibrosis at Day 14 in the bleomycin model (Figure 8F).

***Human single-cell RNA sequencing data and IF staining validates mouse studies.*** Tissue from patients with IPF and healthy control patients was co-stained for CDH5 and S1pr1 (Figure 9A). Similar to the bleomycin mouse images, we found areas with reduced CDH5 staining and S1pr1 staining in the lungs of patients with IPF as compared with normal healthy controls, and these areas appeared to be the more fibrotic regions (Figure 9A, white box). Interestingly, S1P levels from plasma of patients with IPF were increased compared with levels from plasma of healthy control patients (Figure 9B). Two recent single-cell RNA sequencing papers profiled cells in the lungs of patients with IPF at the time of lung transplantation (18, 19). From these data (GSE135893, GSE136831), we extracted cells annotated as vascular endothelial cells (vEC) and performed clustering using Seurat (17). Five vEC clusters emerged with correspondence to populations described by Travaglini and colleagues (27) as arterial (Art; *DKK2*$^+$), venous (Vn; *CPE*$^+$), peri-bronchial (Bronch; *PLVAP*$^+$), capillary (Cap; *IL7R*$^+$), and capillary-a (Cap-a; *EDNRB*$^+$) (Figure E6). Analysis of *S1pr1* transcript levels revealed reduced expression in IPF, specifically in the two subtypes of lung capillary cells, Cap and Cap-a (Figure 9C).

## Discussion

Pulmonary fibrosis is thought to result from aberrant wound healing responses to repetitive lung injury. Increased vascular permeability is a critical component of wound healing following injury (5). There is growing evidence demonstrating a correlation between increased vascular permeability in the lungs and the development of pulmonary fibrosis (28); however, a causal relationship has not been established. In the studies presented here, we demonstrate that genetic disruption of endothelial *S1pr1* expression led to an increase in vascular permeability and exacerbation of the fibrotic response to bleomycin-induced lung injury. We also found increased immune cell infiltration in the BAL fluid of EC-*S1pr1*$^{-/-}$ mice and increased intraalveolar coagulation with increases in D-dimer in both the BAL fluid and the lung tissue. Our data support the hypothesis that persistent vascular hyperpermeability could promote fibrogenesis rather than normal wound repair and suggests that targeting vascular permeability could be an effective and novel therapeutic strategy for pulmonary fibrosis.

Signaling of the bioactive lipid S1P through its various GPCRs, S1PR1–5, has been implicated in the development of pulmonary fibrosis (12, 22, 29, 30). S1P levels have been shown to be elevated in serum and BAL fluid from patients with IPF (11). Mice deficient in endothelial S1PR1 have recently been shown to have increased vascular leak and pulmonary fibrosis after hydrochloric acid injury (26). In addition, one of the enzymes that generates S1P, sphingosine kinase-1 (SPHK1), was found to have elevated levels in the lung tissue of patients with IPF (11). In another aptamer-based proteomics analysis, SPHK1 was one of the top 10 most significantly up-regulated proteins in the serum and BAL of patients with IPF (31). In contrast, global, fibroblast-specific, and epithelial-specific *SphK1* deletion mice all showed reduced fibrosis after IT bleomycin (29, 32). However, mice deficient in *SphK1* in endothelial cells had increased lung injury and fibrosis after bleomycin challenge (32).

Patients with IPF have increased pulmonary vascular permeability as quantified by protein permeability indices, and the degree of permeability correlates with mortality (6). Studies using inhaled $^{99m}$Tc-DTPA have also shown increased permeability in the lungs of IPF patients (7, 33). Recently, we demonstrated that IPF patients have increased vascular permeability as measured by extravasation of an albumin-labeled gadolinium probe using lung MRI (8). It is interesting to note that the patients in this MRI study were imaged during the routine course of their disease and not during acute exacerbations, suggesting that an underlying increase in vascular permeability in patients with IPF may contribute to the progressive development of fibrosis.

In the studies presented here, we found that disruption of endothelial S1P/S1PR1 signaling leads to increased vascular permeability. This defect in endothelial barrier function is present at baseline but is exacerbated in the context of lung injury. This fits with previously published data that S1P signaling through its G-protein coupled receptor (GPCR) S1PR1 at the cell surface reduces vascular permeability through the establishment of subsurface cortical actin rings which enhance intercellular junctions and barrier function (10, 34, 35). Indeed, the administration of S1P in a mouse model of acute lung injury was able to reverse lipopolysaccharide (LPS) induced vascular leak (36). We demonstrated previously that administration of the S1P receptor modulator FTY-720 in conjunction with a very low dose of IT bleomycin resulted in increased vascular permeability and subsequent pulmonary fibrosis (12). The mechanism of functional antagonism seen with FTY-720 involves the phosphorylation and ubiquitylation of S1PR1 following binding with FTY-720. This ubiquitylation targets the S1PR1 receptor for degradation rather than its normal recycling back to the cell surface of the endothelial cell, which is seen after endogenous binding of S1P (37).

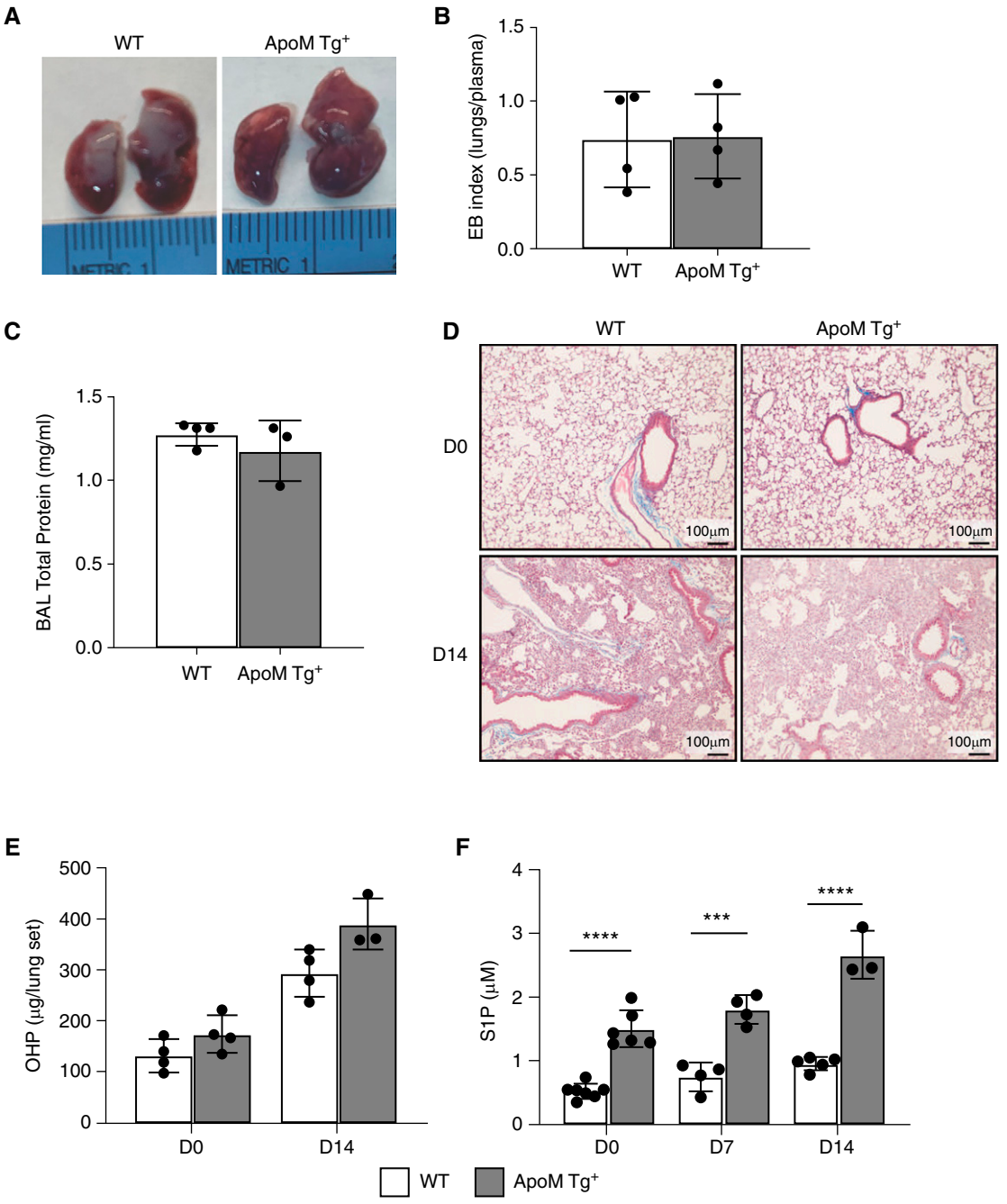


**Figure 8.** Increased circulating S1P is insufficient to protect mice from bleomycin-induced pulmonary fibrosis. (*A*) Transgenic mice overexpressing human apolipoprotein M (ApoM $Tg^+$) were bred, and Evans blue dye assay was performed at Day 7 after standard-dose IT bleomycin. (*B*) Evans blue indices were calculated using Evans blue dye indices in the lungs and plasma of ApoM $Tg^+$ mice and littermate controls (WT). $n = 4$ mice per group. (*C*) BAL total protein was quantified at Day 14 after standard dose bleomycin. (*D*) Histology at Days 0 and 14 after standard-dose IT bleomycin were stained with hematoxylin and eosin and Masson's trichrome staining. Representative images are shown from $n = 3$ mice per group. Scale bars, 100 μm. (*E*) Quantification of fibrosis was performed with hydroxyproline assay. (*F*) S1P levels were quantified by mass spectrometry from circulating plasma at baseline (Day 0), Day 7, and Day 14 after standard-dose bleomycin. $n = 3$–6 mice per group. $n = 3$–8 mice per group. $^{***}P < 0.001$, and $^{****}P < 0.0001$ for comparisons of S1P between ApoM-$Tg^+$ and control mice.

We also demonstrate that endothelial-specific deletion of *S1pr1* leads to exaggerated pulmonary fibrosis after low-dose IT bleomycin challenge. This is associated with increased coagulation in the lung and airspaces following injury and an increase in immune cell infiltration at one week after injury in the EC-*S1pr1*$^{-/-}$ mice. IPF patients have also increased intraalveolar coagulation as quantified by BAL tissue factor levels (38). Intraalveolar coagulation leads to fibrin deposition, which provides a provisional matrix in the alveolar space upon which collagen deposits and matures, creating more permanent fibrotic scars. In

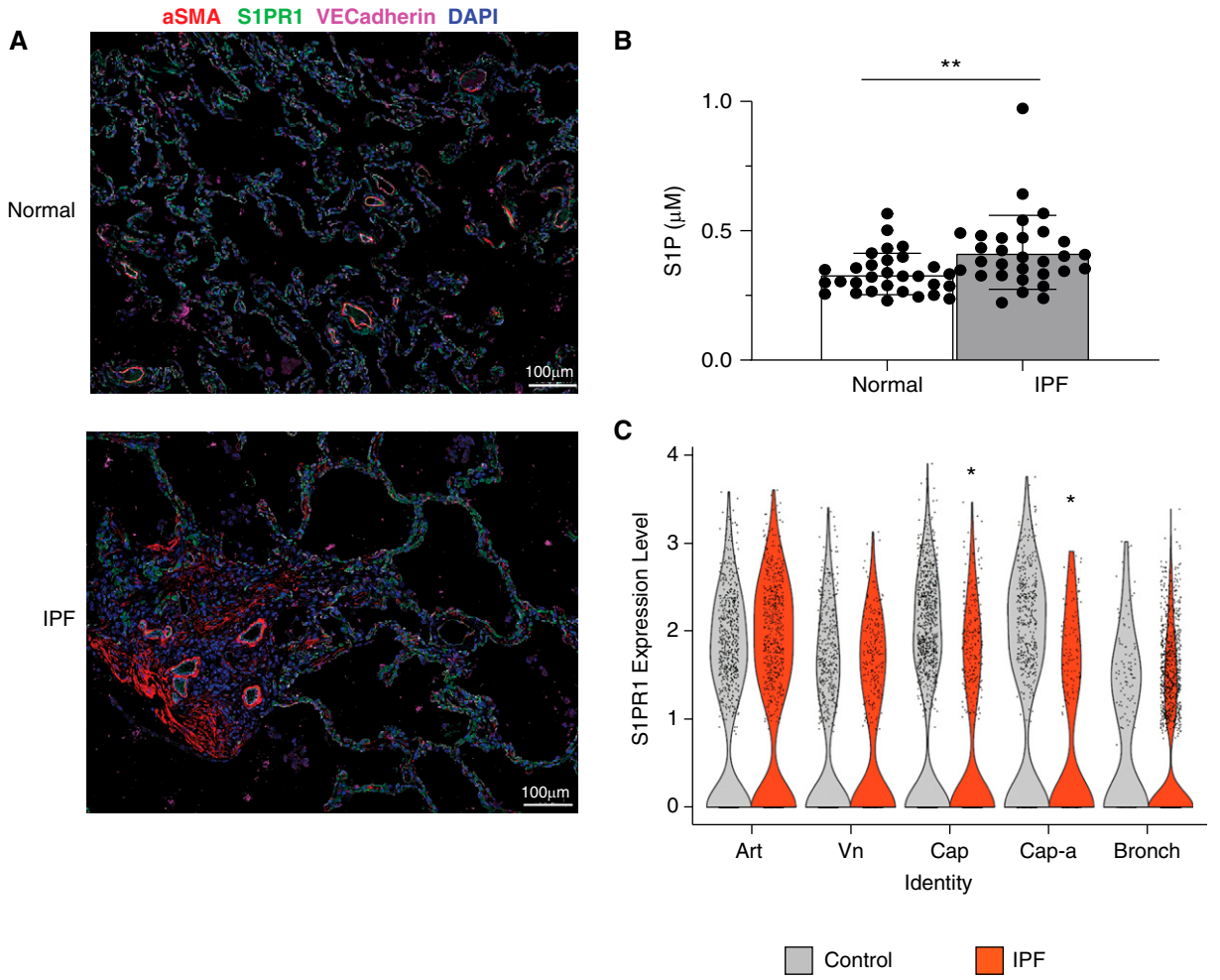


| Vessel | Art | Vn | Cap | Cap-a | Bronch |
|---|---|---|---|---|---|
| P-value | 0.289 | 0.404 | 0.011 | 0.002 | 0.38 |
| FC | 1.16 | 0.913 | 0.651 | 0.53 | 0.843 |

**Figure 9.** Clinical relevance of *S1pr1* modulation in pulmonary fibrosis. (*A*) Lung tissue from patients with idiopathic pulmonary fibrosis (IPF) and healthy age-matched controls were stained for endothelial marker VE-Cadherin and S1PR1. White box indicates an area of fibrosis. Scale bars, 100 μm. (*B*) Plasma from patients with IPF and sex- and age-matched healthy controls were analyzed by mass spectrometry to quantify S1P levels. $n = 30$ patients per group. (*C*) Violin plot of *S1PR1* expression in subtypes of lung vascular endothelial cells from 38 control donors (3,458 total cells; 2,458 cells from Kropski paper, 1,000 cells from Kaminski paper) and 44 IPF patients (3,663 total cells; 1,720 cells from Kropski paper, 1,943 cells from Kaminski paper). Cells from scRNA-seq accessions GSE135893 and GSE136831 were merged and re-clustered (*see* supplemental Figure E6). Fold-change values indicate the expression ratio of [IPF/Control]. *See* Figure E6. *$P > 0.05$ and **$P > 0.01$.
Art = artery; Bronch = bronchial; Cap = capillary; Cap-a = capillary A; FC = fold change; Vn = vein.

this study we found increased D-dimer levels in the BAL and lung tissue of EC-*S1pr1*$^{-/-}$ mice after low-dose bleomycin challenge. We have previously shown that D-dimer levels in the lung tissue correlate with fibrin deposition identified by molecular imaging using a fibrin-targeted contrast agent for MRI (23). Furthermore, we have demonstrated that leakage of procoagulant proteins such as thrombin into the alveolar spaces contributes to fibrosis through other mechanisms beyond facilitating matrix deposition. In addition to its procoagulant functions, thrombin signals through the protease-activated receptor-1 (PAR-1) receptors on alveolar epithelial cells to induce αvβ6 integrin expression, also on epithelial cells, and ultimately drives TGFβ activation on fibroblasts (23). Therefore, vascular permeability in the context of lung injury permits the leakage of prothrombotic and profibrotic mediators into the alveolar spaces, where they are normally not present at high concentrations. Similarly, vascular permeability in the context of injury permits the leakage of profibrotic immune cells into the alveolar spaces. Although immunosuppressive medications have thus far failed to demonstrate clinical efficacy in IPF patients, recent studies have shown that both the innate and adaptive immune system play roles in promoting pulmonary fibrosis (39). Macrophages have been shown to

produce soluble mediators such as TGFβ, which activate fibroblasts. Increases in T cell subsets and activation have been shown in lung tissue and BAL from patients with IPF (12, 40). These data suggest that the increased permeability induced by disrupted *S1pr1* signaling facilitates a pro-fibrotic environment by allowing the influx of both immune cells and profibrotic proteins into the airspaces.

In addition to the effect that permeability has on extravascular coagulation and immune cell infiltration, evidence has been accumulating that endothelial defects are linked to other established mechanisms of fibrogenesis. For example, it was recently shown that aged mice who have undergone lung injury with hydrochloric acid have increased vascular permeability, but also decreased regeneration of alveolar type 1 cells, decreased proliferation of alveolar type 2 cells, and increased myfibroblast activation (26). The hypothesis from this data was that increased permeability in the context of injury allowed profibrotic mediators to enter the lung and activate perivcascular fibroblasts. In addition, given the beneficial effect on epithelial cell repair after injury, there may be cell–cell interactions that are affected indirectly by S1P/S1PR1 signaling in the endothelium.

We saw a reduction in total $CD31^+$ endothelial cells and total S1PR1 protein expression in the lungs of mice after bleomycin lung injury. This is consistent with results shown by others in mouse models of lung injury and fibrosis. It was recently demonstrated that aging suppresses endothelial S1PR1 expression, which is associated with increased fibrosis after acid injury (26). Consistent with our results, in addition, this group demonstrated that EC S1PR1 knockout mice have increased vascular permeability and fibrosis after hydrochloric acid–induced lung injury as compared with intact littermate controls, mirroring the effect of aging. We also saw an increase in S1P levels in the plasma of patients with IPF as compared with healthy controls, which is consistent with previously published data (11). We did not see the same increase in the bleomycin model, which differs from previously published data, and could be explained by our measurements in plasma as compared with previously measured levels in lung tissue, or by differences in bleomycin dose (29). Using recently published single cell RNA sequencing data, we found decreased *S1pr1* expression in two types of capillary endothelial cell populations. We also demonstrated this by immunoflouresnce using tissue from explanted lung of IPF patients.

Interestingly, EC-$S1pr1^{-/-}$ mice without lung injury did not have increased fibrosis even up to 6 months after deletion, despite ongoing enhanced vascular permeability. This supports the concept that increased vascular permeability alone is not enough to promote fibrosis without a second injury stimulus. Our data suggest that the integrity of the vasculature is an important factor in determining whether the tissue environment is profibrotic or not. In this case, increased permeability alone, or low-level bleomycin alone, were both inadequate to promote fibrosis, but the combination exaggerated the fibrotic response to injury. It may follow that some patients have a defect in vascular integrity that predispose them to fibrosis in the context of a low-level injury, such as from inhaled toxins or viral infections. An additional hypothesis has been explored recently demonstrating a reduction in S1P/S1PR1 signaling and ApoM production with aging in mouse models of pulmonary and liver fibrosis (26).

We used ApoM $Tg^+$ mice in these studies, which had threefold increased circulating S1P, but did not demonstrate protection against fibrosis in the context of bleomycin lung injury. These data suggest that elevating circulating S1P levels alone is insufficient to protect against fibrosis in the context of a severe lung injury such as bleomycin. There are several possible explanations for this, including the possibility that there is already saturation of S1P/S1PR1 interactions, such that further augmentation of circulating S1P levels does not increase S1PR1 activation further. It is also possible that ApoM $Tg^+$ mice are adapted to higher S1P levels, or other EC protective pathways, such as Angiopoietin/Tie2 signaling, may need to be engaged as well. Another potential explanation is that bleomycin suppresses autocrine S1P signaling, including *SphK1*, *Spns2*, and *S1pr1* pathways. Alternatively, S1P may have profibrotic effects on other cell types, such as fibroblasts, so although there may be a barrier protective effect of S1P on endothelial cells, the net result of increased circulating S1P is not antifibrotic (41). While these results are interesting, they do not necessarily mean that therapeutic dosing of an S1PR1 agonist will be ineffective, and the potential of S1PR1 agonism as a therapeutic target should be further studied.

There are several S1PR1 modulators currently available, with many of them appearing to function as functional antagonists of the receptor with prolonged exposure (37). However, our data would suggest that agonism of S1PR1 through enhanced expression or function on endothelial cells could be a novel and effective antifibrotic strategy. Further studies are needed to investigate the role of sphingolipid signaling and S1PR1 receptor expression in IPF patients and to determine the therapeutic potential of receptor agonism in the clinical setting. In addition, our data supports an important link between the endothelium and the development of pulmonary fibrosis. Specifically, targeting endothelial injury and vascular permeability may have the ability to provide a novel therapeutic strategy for IPF and for other fibrosing diseases, especially those induced by acute injury such as post-acute respiratory distress syndrome fibrosis. ■

**Author disclosures** are available with the text of this article at www.atsjournals.org

**Acknowledgment:** The authors gratefully acknowledge Dr. Andrew M. Tager, who inspired these studies but passed away before the manuscript was completed. They also thank Susan Sheng, Ph.D., from the Division of Pulmonary and Critical Care Medicine at Massachusetts General Hospital for helping with review and revision of the manuscript.

## References

1. Raghu G, Weycker D, Edelsberg J, Bradford WZ, Oster G. Incidence and prevalence of idiopathic pulmonary fibrosis. *Am J Respir Crit Care Med* 2006;174:810–816.

2. King TE Jr, Bradford WZ, Castro-Bernardini S, Fagan EA, Glaspole I, Glassberg MK, *et al.*; ASCEND Study Group. A phase 3 trial of pirfenidone in patients with idiopathic pulmonary fibrosis. *N Engl J Med* 2014;370:2083–2092.

3. Richeldi L, du Bois RM, Raghu G, Azuma A, Brown KK, Costabel U, *et al.*; INPULSIS Trial Investigators. Efficacy and safety of nintedanib in idiopathic pulmonary fibrosis. *N Engl J Med* 2014;370: 2071–2082.
4. Selman M, King TE, Pardo A; American Thoracic Society; European Respiratory Society; American College of Chest Physicians. Idiopathic pulmonary fibrosis: prevailing and evolving hypotheses about its pathogenesis and implications for therapy. *Ann Intern Med* 2001;134: 136–151.
5. Brown LF, Dvorak AM, Dvorak HF. Leaky vessels, fibrin deposition, and fibrosis: a sequence of events common to solid tumors and to many other types of disease. *Am Rev Respir Dis* 1989;140: 1104–1107.
6. McKeown S, Richter AG, O'Kane C, McAuley DF, Thickett DR. MMP expression and abnormal lung permeability are important determinants of outcome in IPF. *Eur Respir J* 2009;33:77–84.
7. Mogulkoc N, Brutsche MH, Bishop PW, Murby B, Greaves MS, Horrocks AW, *et al.*; Greater Manchester Pulmonary Fibrosis Consortium. Pulmonary (99m)Tc-DTPA aerosol clearance and survival in usual interstitial pneumonia (UIP). *Thorax* 2001;56:916–923.
8. Montesi SB, Rao R, Liang LL, Goulart HE, Sharma A, Digumarthy SR, *et al.* Gadofosveset-enhanced lung magnetic resonance imaging to detect ongoing vascular leak in pulmonary fibrosis. *Eur Respir J* 2018;51:1800171.
9. Kawanami O, Matsuda K, Yoneyama H, Ferrans VJ, Crystal RG. Endothelial fenestration of the alveolar capillaries in interstitial fibrotic lung diseases. *Acta Pathol Jpn* 1992;42:177–184.
10. Dudek SM, Garcia JG. Cytoskeletal regulation of pulmonary vascular permeability. *J Appl Physiol (1985)* 2001;91:1487–1500.
11. Milara J, Navarro R, Juan G, Peiró T, Serrano A, Ramón M, *et al.* Sphingosine-1-phosphate is increased in patients with idiopathic pulmonary fibrosis and mediates epithelial to mesenchymal transition. *Thorax* 2012;67:147–156.
12. Shea BS, Brooks SF, Fontaine BA, Chun J, Luster AD, Tager AM, *et al.* Prolonged exposure to sphingosine 1-phosphate receptor-1 agonists exacerbates vascular leak, fibrosis, and mortality after lung injury. *Am J Respir Cell Mol Biol* 43; 662–673.
13. Camerer E, Regard JB, Cornelissen I, Srinivasan Y, Duong DN, Palmer D, *et al.* Sphingosine-1-phosphate in the plasma compartment regulates basal and inflammation-induced vascular leak in mice. *J Clin Invest* 2009;119:1871–1879.
14. Choi JW, Gardell SE, Herr DR, Rivera R, Lee CW, Noguchi K, *et al.* FTY720 (fingolimod) efficacy in an animal model of multiple sclerosis requires astrocyte sphingosine 1-phosphate receptor 1 (S1P1) modulation. *Proc Natl Acad Sci USA* 2011;108:751–756.
15. Pitulescu ME, Schmidt I, Benedito R, Adams RH. Inducible gene targeting in the neonatal vasculature and analysis of retinal angiogenesis in mice. *Nat Protoc* 2010;5:1518–1534.
16. Christoffersen C, Jauhiainen M, Moser M, Porse B, Ehnholm C, Boesl M, *et al.* Effect of apolipoprotein M on high density lipoprotein metabolism and atherosclerosis in low density lipoprotein receptor knock-out mice. *J Biol Chem* 2008;283:1839–1847.
17. Stuart T, Butler A, Hoffman P, Hafemeister C, Papalexi E, Mauck WMP 3rd, *et al.* Comprehensive integration of single-cell data. *Cell* 2019;177: 1888–1902.
18. Habermann AC, Gutierrez AJ, Bui LT, Yahn SL, Winter NI, Calvi CL, *et al.* Single-cell RNA sequencing reveals profibrotic roles of distinct epithelial and mesenchymal lineages in pulmonary fibrosis. *Sci Adv* 2020;6:eaba1972.
19. Adams TS, Schupp JC, Poli S, Ayaub EA, Neumark N, Ahangari F, *et al.* Single-cell RNA-seq reveals ectopic and aberrant lung-resident cell populations in idiopathic pulmonary fibrosis. *Sci Adv* 2020;6: eaba1983.
20. Tager AM, LaCamera P, Shea BS, Campanella GS, Selman M, Zhao Z, *et al.* The lysophosphatidic acid receptor LPA1 links pulmonary fibrosis to lung injury by mediating fibroblast recruitment and vascular leak. *Nat Med* 2008;14:45–54.
21. Obinata H, Kuo A, Wada Y, Swendeman S, Liu CH, Blaho VA, *et al.* Identification of ApoA4 as a sphingosine 1-phosphate chaperone in ApoM- and albumin-deficient mice. *J Lipid Res* 2019;60:1912–1921.
22. Swendeman SL, Xiong Y, Cantalupo A, Yuan H, Burg N, Hisan Y, et al. An engineered S1P chaperone attenuates hypertension and ischemic injury. *Sci Signal* 2017;10(492):eaal2722.
23. Shea BS, Probst CK, Brazee PL, Rotile NJ, Blasi F, Weinreb PH, *et al.* Uncoupling of the profibrotic and hemostatic effects of thrombin in lung fibrosis. *JCI Insight* 2017;2:86608.
24. Krump-Konvalinkova V, Yasuda S, Rubic T, Makarova N, Mages J, Erl W, *et al.* Stable knock-down of the sphingosine 1-phosphate receptor S1P1 influences multiple functions of human endothelial cells. *Arterioscler Thromb Vasc Biol* 2005;25:546–552.
25. Cao Z, Lis R, Ginsberg M, Chavez D, Shido K, Rabbany SY, *et al.* Targeting of the pulmonary capillary vascular niche promotes lung alveolar repair and ameliorates fibrosis. *Nat Med* 2016;22:154–162.
26. Ding BS, Yang D, Swendeman SL, Christoffersen C, Nielsen LB, Friedman SL, *et al.* Aging suppresses sphingosine-1-phosphate chaperone ApoM in circulation resulting in maladaptive organ repair. *Dev Cell* 2020;53:677–690.e4.
27. Travaglini KJ, Nabhan AN, Penland L, Sinha R, Gillich A, Sit RV, *et al.* A molecular cell atlas of the human lung from single-cell RNA sequencing. *Nature* 2020;587:619–625.
28. Probst CK, Montesi SB, Medoff BD, Shea BS, Knipe RS. Vascular permeability in the fibrotic lung. *Eur Respir J* 2020; 56:1900100.
29. Huang LS, Berdyshev E, Mathew B, Fu P, Gorshkova IA, He D, *et al.* Targeting sphingosine kinase 1 attenuates bleomycin-induced pulmonary fibrosis. *FASEB J* 2013;27:1749–1760.
30. Todd JL, Neely ML, Overton R, Durham K, Gulati M, Huang H, *et al.*; IPF-PRO Registry investigators. Peripheral blood proteomic profiling of idiopathic pulmonary fibrosis biomarkers in the multicentre IPF-PRO Registry. *Respir Res* 2019;20:227.
31. O'Dwyer DN, Norman KC, Xia M, Huang Y, Gurczynski SJ, Ashley SL, *et al.* The peripheral blood proteome signature of idiopathic pulmonary fibrosis is distinct from normal and is associated with novel immunological processes. *Sci Rep* 2017;7:46560.
32. Huang LS, Sudhadevi T, Fu P, Punathil-Kannan PK, Ebenezer DL, Ramchandran R, *et al.* Sphingosine kinase 1/S1P signaling contributes to pulmonary fibrosis by activating Hippo/YAP pathway and mitochondrial reactive oxygen species in lung fibroblasts. *Int J Mol Sci* 2020;21:E2064.
33. Wells AU, Hansell DM, Harrison NK, Lawrence R, Black CM, du Bois RM. Clearance of inhaled 99mTc-DTPA predicts the clinical course of fibrosing alveolitis. *Eur Respir J* 1993;6:797–802.
34. Garcia JG, Liu F, Verin AD, Birukova A, Dechert MA, Gerthoffer WT, *et al.* Sphingosine 1-phosphate promotes endothelial cell barrier integrity by Edg-dependent cytoskeletal rearrangement. *J Clin Invest* 2001;108:689–701.
35. Schaphorst KL, Chiang E, Jacobs KN, Zaiman A, Natarajan V, Wigley F, *et al.* Role of sphingosine-1 phosphate in the enhancement of endothelial barrier integrity by platelet-released products. *Am J Physiol Lung Cell Mol Physiol* 2003;285:L258–L267.
36. Peng X, Hassoun PM, Sammani S, McVerry BJ, Burne MJ, Rabb H, *et al.* Protective effects of sphingosine 1-phosphate in murine endotoxin-induced inflammatory lung injury. *Am J Respir Crit Care Med* 2004; 169:1245–1251.
37. Oo ML, Chang SH, Thangada S, Wu MT, Rezaul K, Blaho V, *et al.* Engagement of $S1P_1$-degradative mechanisms leads to vascular leak in mice. *J Clin Invest* 2011;121:2290–2300.
38. Kotani I, Sato A, Hayakawa H, Urano T, Takada Y, Takada A. Increased procoagulant and antifibrinolytic activities in the lungs with idiopathic pulmonary fibrosis. *Thromb Res* 1995;77:493–504.
39. Desai O, Winkler J, Minasyan M, Herzog EL. The role of immune and inflammatory cells in idiopathic pulmonary fibrosis. *Front Med (Lausanne)* 2018;5:43.
40. Nuovo GJ, Hagood JS, Magro CM, Chin N, Kapil R, Davis L, *et al.* The distribution of immunomodulatory cells in the lungs of patients with idiopathic pulmonary fibrosis. *Mod Pathol* 2012; 25:416–433.
41. Sobel K, Menyhart K, Killer N, Renault B, Bauer Y, Studer R, *et al.* Sphingosine 1-phosphate (S1P) receptor agonists mediate pro-fibrotic responses in normal human lung fibroblasts via S1P2 and S1P3 receptors and Smad-independent signaling. *J Biol Chem* 2013;288: 14839–14851.